

Exciton–polariton transition induced by elastic exciton–exciton collisions in ultra-high quality AlGaAs alloys

© T.S. Shamirzaev[¶], A.I. Toropov, A.K. Bakarov, K.S. Zhuravlev, A.Yu. Kobitski*, H.P. Wagner*, D.R.T. Zahn*

Institute of Semiconductor Physics,
630090 Novosibirsk, Russia

* Institut für Physik, TU Chemnitz,
D-09107 Chemnitz, Deutschland

(Получена 19 сентября 2005 г. Принята к печати 10 октября 2005 г.)

The stationary and time-resolved polariton radiation in ultra-high quality AlGaAs layers have studied. It has been found that elastic exciton–exciton collisions lead to the appearance of a low-energy line of the polariton radiation. We show that the rate of the exciton-to-polariton transitions caused by elastic exciton–exciton collisions is determined not only by the density of the excitonic gas but also by its temperature which is in accordance to existing theoretical predictions.

PACS: 71.35.+z, 71.36.+c, 71.38.+i

1. Introduction

It is well known that the exciton–photon coupling leads to the creation of exciton polaritons, which are new elementary excitations of the crystalline semiconductor [1,2]. Under non-resonant excitation the exciton polaritons are generated with a high momentum (k) on the lower polariton branch (LPB) of the dispersion curve [3]. Subsequently the polaritons relax in energy and momentum due to their interaction with phonons and finally escape from the crystal. Already the first studies of exciton polaritons have shown that the spectrum of the polariton radiation is determined by their spatial and energy distribution [4–6]. It was established, that the decrease of the radiative lifetime and the exciton–phonon scattering rate with decreasing polariton momentum results in a bottleneck effect, which has been theoretically predicted by Toyozawa [6] and has been experimentally observed later by many groups [7–12]. The bottleneck in the relaxation process leads to a strong nonequilibrium energy distribution of polaritons so that the concentration of particles with a momentum $k < k_0$ (where k_0 is the momentum value at the crossover between excitons and photons on the dispersion curve) is smaller than the concentration of the particles with a momentum $k > k_0$. In the following, we refer to polaritons as particles with $k < k_0$, and to excitons as particles with $k > k_0$.

By now, experimental and theoretical studies of the formation and evolution of the energy distribution of exciton polaritons at low and high levels of non-resonant optical excitation have been performed [4–14]. At low excitation levels the energy distribution of exciton polaritons is determined by collisions (both elastic and inelastic) of excitons with impurities and phonons [13]. Due to the small rate of the exciton-to-polariton transitions the polariton concentration is very low in this case. At high excitation levels, the energy distribution of the exciton polaritons is determined by the inelastic exciton–exciton

scattering, which leads to a high rate of the exciton-to-polariton transitions [14]. The case of an intermediate level of optical excitation where the energy distribution of the exciton polaritons (and therefore, the spectrum of the polariton radiation) is determined by elastic exciton–exciton collisions has not been experimentally studied yet. According to theoretical predictions by Bisti [15] an elastic collision of two excitons results in a relaxation of one of them into a polariton and a transition of the second exciton into the high-momentum region of the LPB. This should lead to the appearance of an additional polariton luminescence line that is red-shifted from the free exciton transition. Up to now such a line has not been observed experimentally. The main obstacle for an experimental observation of this line is its masking by the impurity-bound exciton lines, which are usually present in the near-bandgap luminescence of semiconductor crystals.

Recently, we reported on the growth of ultra-high quality $\text{Al}_x\text{Ga}_{1-x}\text{As}$ layers by molecular beam epitaxy [16]. The thin X line of the free exciton radiation dominates the luminescence spectra of these layers, whereas the bound exciton lines are absent. Therefore, this layers was the good object to search the new line of LPB predicted by Bisti [15]. It is necessary to note that in spite of the theory of bulk polaritons is based on models of uniform media or crystals, but one could argue that neither uniformity, nor crystal structure of a substance are necessary for polaritons to occur. As an example one can refer to existence of the polaritons associated with quasi-2D excitons in quantum-size heterostructures. As another example, in spite of opinion that excitonic polariton does not occur in solid solution we demonstrated recently excitonic polariton controlled low temperature the optical absorption in our $\text{Al}_x\text{Ga}_{1-x}\text{As}$ layers up to temperatures 155 K [17].

In this paper, we report on the experimental observation of a new polaritonic luminescence line, which is due to elastic exciton–exciton collisions in ultra-high quality AlGaAs layers. It is shown that the rate of the exciton–polariton transitions caused by elastic exciton–exciton collisions is

[¶] E-mail: timur@thermo.isp.nsc.ru
Fax: 8-383-3332771

determined not only by the density of the exciton gas but also by its temperature, in accordance to theoretical predictions by Bisti [15].

2. Experimental

The studied layers of ultra-high quality $\text{Al}_x\text{Ga}_{1-x}\text{As}$ with AlAs fractions of $x = 0.21$ and $x = 0.26$ were obtained by molecular beam epitaxy. The details of the layer growth and the equipment used for the recording of continuous wave (*cw*) photoluminescence (PL) were described elsewhere [16]. The *cw* PL was excited using an Ar-ion laser with a wavelength of 488 nm. The excitation power density was changed from $3 \cdot 10^{-4}$ to 400 W/cm^2 using neutral density filters. The time-resolved PL was excited using a dye laser synchronously pumped by a mode-locked Ar-ion laser. This resulted in about 20 ps duration pulses at a wavelength of 580 nm. The intrinsic repetition rate of 80 MHz set by the Ar-ion laser cavity length was reduced to 4 MHz using a cavity damper. The PL was analyzed using a CROMEX 250IS spectrometer and detected by a Hamamatsu C4334 Streakscope camera. The time resolution of the system was better than 50 ps. Samples were placed in a closed-cycle CTI-Cryogenics cryostat. The laser spot focused on the sample had a Gaussian shape with a half-width of $250 \mu\text{m}$ during both the *cw* and time-resolved measurements. The image of the excited spot was projected onto the entrance slit of the monochromator with a unity magnification. Since the monochromator slit widths of $10\text{--}20 \mu\text{m}$ were used, the data were recorded with a quasi-uniform excitation.

3. Experimental results

Fig. 1 shows the 4.2 K photoluminescence spectra of the $\text{Al}_x\text{Ga}_{1-x}\text{As}$ layer with an AlAs fraction of $x = 0.21$ measured at different excitation levels. The line labeled X dominates in all spectra. Recently, we have shown that the PL maximum of the X line coincides with the transmission minimum [16] allowing to attribute this line to the lower polariton branch radiation [18]. The line which is related to the radiation of the upper polariton branch is absent in the spectra, which evidences the ultra-low concentration of shallow donors in the layer [19]. A new line labeled Y appears on the low-energy tail of the X line when the excitation power exceeds 0.5 mW [20]. This Y line shifts towards lower energy when the excitation power is increased. The variation of the relative position of the Y line with respect to the X line as a function of the laser power is depicted in Fig. 2 for layers with AlAs fractions $x = 0.21$ and $x = 0.26$. The dependence of the Y line position on the laser power shows a nonlinear behavior with a maximum energy shift of 9 meV. The relative peak intensity of the Y line remains nearly constant when the excitation power is increased from 0.5 to 10 mW, whereas it decreases when the excitation power exceeds 10 mW as

shown in Fig. 3. Fig. 4, *a* demonstrates the PL kinetics of the X and Y lines after the pulsed laser excitation with a pulse energy of 2 nJ. The intensities of both lines increase within the initial 200 ps after the excitation pulse. This initial rise time is attributed to the exciton creation and

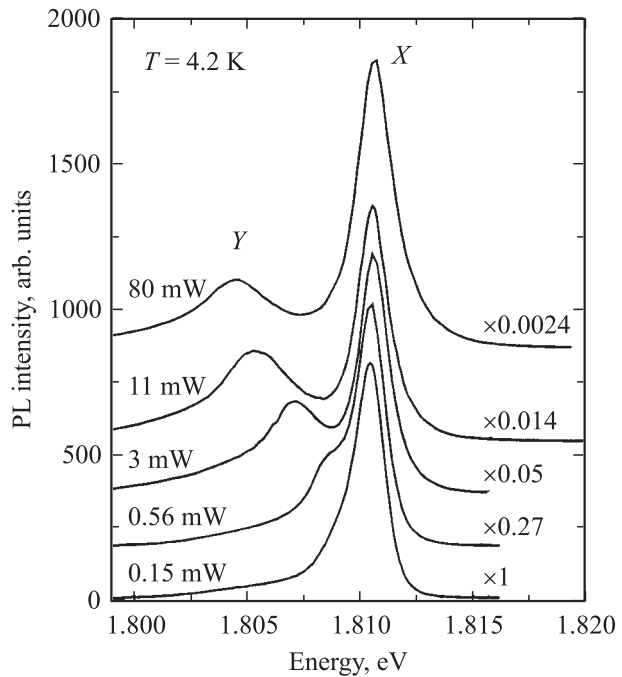


Figure 1. Low-temperature ($T = 4.2 \text{ K}$) photoluminescence spectra of a pure $\text{Al}_x\text{Ga}_{1-x}\text{As}$ layer with the AlAs fraction $x = 0.21$ measured at different excitation powers, which are labeled in the figure.

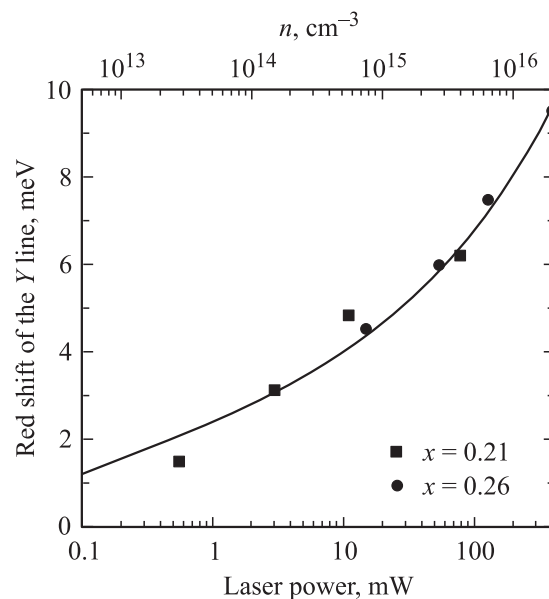


Figure 2. The red shift of the Y line as a function of excitation power in $\text{Al}_x\text{Ga}_{1-x}\text{As}$ layers with AlAs fractions of $x = 0.21$ and $x = 0.26$. The calculated energy shift of the maximum position of the Y line is given as a solid line.

energy relaxation [21–24]. Thereby after the end of the excitation pulse the Y line intensity increases more rapidly than that of the X line, while the decay of both lines starts simultaneously. In addition oscillations are observed at the beginning of the decay curves. The amplitude of these oscillations diminishes when the excitation power is reduced and the oscillations disappear when the pulse energy is lower than 0.2 nJ as shown in Fig. 4, *b*. The origin of these oscillations which is not yet understood might be attributed to a spatial variation of the excitonic gas density [25]. The decay curve of the X emission is expressed by an exponential function with a decay time of 1090 ps. The decay of the Y line shows a biexponential behavior where the fast initial dynamics has a decay time of 170 ps followed by a slower decay rate with a time constant of 510 ps. When the excitation density is decreased the kinetics of the Y line changes. At excitation densities lower than 0.2 nJ the decay of the Y line becomes single exponential with a decay time of 510 ps.

4. Discussion

4.1. Identification of the Y line

There are several possibilities of explain an emission line on the low energy side of the free exciton transition. Such a line can have its origin (i) due to the recombination of bound excitons, (ii) due to phonon replicas of free exciton transitions [26], (iii) or to inelastic exciton–exciton collisions, which result in the so-called P -line [14] and further can be caused (iv) by the recombination of bi- and multi-excitonic molecules, which corresponds to the so-called M -line [14,27]. The nonlinear shift of the Y line with increasing excitation power unambiguously clarifies that this line is not related to impurity bound excitons or

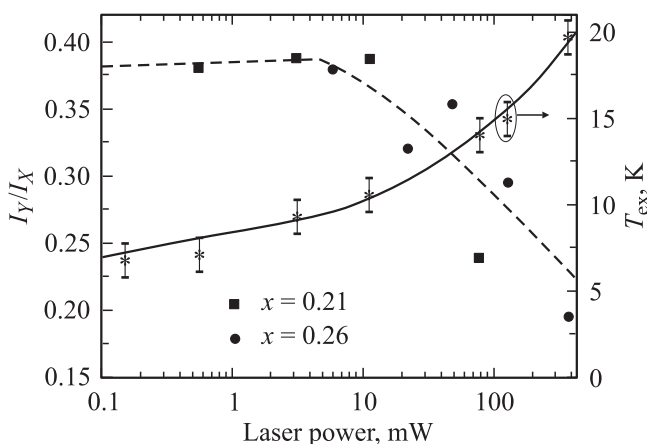


Figure 3. The relative intensity of the Y line as a function of excitation power in $\text{Al}_x\text{Ga}_{1-x}\text{As}$ layers with the AlAs fractions of $x = 0.21$ and $x = 0.26$. The dashed line gives a fitting of the relative Y line intensity by the expression $I_Y/I_X \approx n^{0.1} T_{\text{ex}}^{-5/4}$. The exciton gas temperature T_{ex} as a function of excitation power is expressed by stars. The solid line is given as a guide for the eyes.

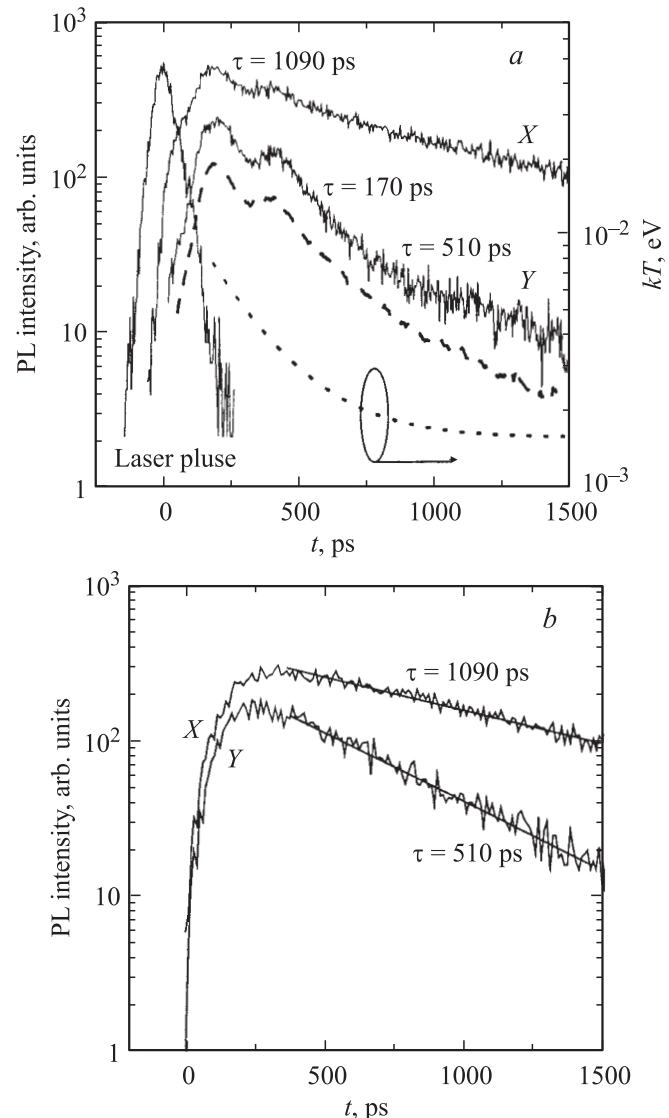


Figure 4. The kinetics of the X and Y line intensity after pulse excitation. The pulse energy was 2 nJ (*a*) and 0.2 nJ (*b*). The thick dashed line is a calculated curve for the additional Y line caused by elastic exciton–exciton collisions. In order to clarify the figure the calculated curve is shifted relative to the experimental data. The time dependence of the exciton gas temperature is shown by the dotted line.

to a phonon replica of the excitonic PL, since the spectral position of these lines is independent on the excitation level. As the energy difference of a P -line to the free exciton transition has a minimum value of 3/4 of the free exciton finding energy being 6 meV in $\text{Al}_x\text{Ga}_{1-x}\text{As}$ with $x = 0.21$ [28] this interpretation is also ruled out. Finally the value of the low energy shift of the Y line is higher than the calculated biexciton binding energy in AlGaAs being 1–2 meV [29,30] at moderate intensities. Moreover, in contrast to the P - and M -lines, the relative intensity of the Y line decreases with increasing excitation power. At the same time, the direction and the nonlinear shift

of the *Y* line with increasing excitation density indicates that this line can be related to a new polariton line, which appears due to elastic exciton–exciton collisions of a portion of excited excitons during their lifetime¹ as predicted by Bisti [15]. The polaritonic picture is suitable in alloys when the probability of polariton decay determined by scattering on impurities and fluctuations of alloy composition is less than the probability of exciton–photon coupling. Since the band gap fluctuations resulting from fluctuations in the alloy composition are the main reason for broadening of the free exciton line [31], we estimated the magnitude of band gap fluctuations from the width of the *X* line. In contrast to A^{II}B^{IV} or A^{III}B^V nitride ternary alloys with a high magnitude of alloy band gap fluctuations [32] the magnitude of alloy fluctuations in the AlGaAs layers is about 1 meV only.

The low values of impurity concentration [16] and alloy potential fluctuations responsible for polariton scattering allow us to suggest that the appearance of the *Y* line can be described in terms of the polaritonic model. Recently, we had a direct experimental evidence of the existence of polaritons in our AlGaAs samples [17]. We have demonstrated that the integrated optical absorption of the free excitons decreases with temperature decrease, which indicates a transition from the excitonic to the polaritonic regime at the lowest temperature.

4.2. Bisti's theory

It is well known that the spectrum of a LPB radiation $I(E)$ which is emitted normal to sample's surface is given by the equation [4,5]:

$$I(E) = TS(E)F(E, z)|_{z=0}\rho(E)v(E), \quad (1)$$

where $TS(E)$ is the transmittance of the surface, $F(E, z)|_{z=0}$ is the distribution function of exciton–polaritons at the surface, $\rho(E)$ and $v(E)$ are the density of excitonic polaritons and their group velocity, respectively. Consequently the exciton–polariton spectrum is determined by its energy and spatial distribution $F(E, z)$ taken at the crystal's surface. In general the distribution function $F(E, z)$ is determined by solving the Boltzmann equation. For low exciton concentration where the exciton scattering is dominated by collisions with impurities and phonons the Boltzmann equation was solved by many groups [4]. It was shown that most of the excitons are concentrated above the crossing point of the excitonic and photonic dispersion curves. Fig. 5 depicts the calculated polariton population which is a product of the distribution function and density of states $\rho(E)F(E, z)|_{z=0}$ as a function of their energy using the model proposed in Ref. 4. The low energy truncation of the exciton–polariton population is a

¹ At intermediate temperatures when both excitons and free electrons are present due to the thermal dissociation of a part of the excitons, a scattering of excitons by electrons should be also considerable. However, we suppose that at lower temperatures, when excitons are not thermally dissociated, the exciton–exciton scattering dominates.

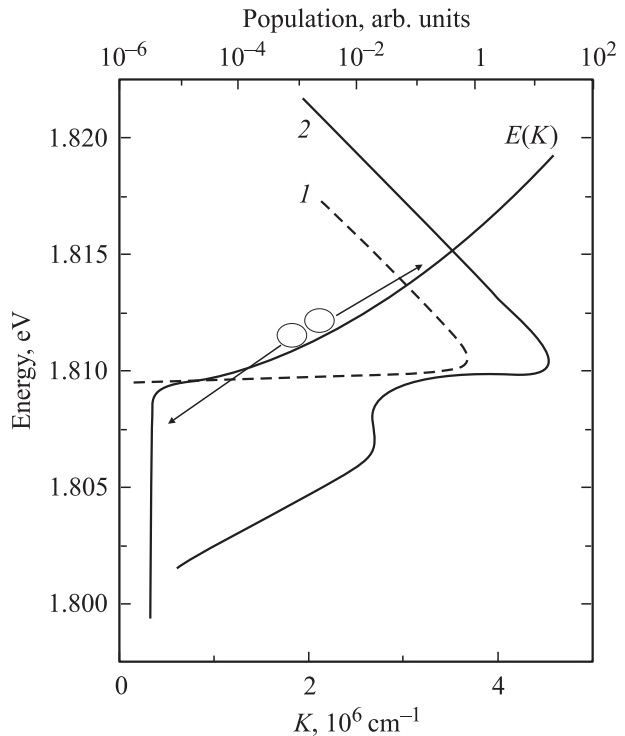


Figure 5. Polariton dispersion curve $E(K)$ for AlGaAs layer with the AlAs fraction of $x = 0.21$. Population of excitonic polaritons as a function of polariton energy calculated according to the models proposed in Ref. 4 (1) and by Bisti (2) at an exciton concentration of $5 \cdot 10^{14} \text{ cm}^{-3}$.

result of the bottleneck in the exciton relaxation process and of the decrease of the polariton escape time in this range. A polaritonic spectrum calculated from Eq. (1) using such an exciton–polariton population exhibits a single line only. In completion to [4,5] Bisti solved the Boltzmann equation for intermediate excitation densities where the exciton scattering is dominated by elastic exciton–exciton collisions. For simplicity exciton–impurity and exciton–phonon scattering have been neglected and a uniform spatial exciton distribution was assumed in these calculations. The calculated exciton–polariton population following Bisti's theory is shown in Fig. 5 as solid curve 2. In the energy range above the crossover point the population obtained by Bisti's approach coincides with that calculated previously, but on the low energy side an additional line appears that is shifted to lower energies compared to the free exciton transition energy. It is important to note that the exciton–exciton collisions become dominant when the probability of these collisions (Γ_{ee}) exceeds the probabilities of the exciton–acoustic phonon (Γ_{ep}), and exciton–impurity scattering processes (Γ_{ei}). A comparison of the values of the Γ_{ep} and Γ_{ee} in GaAs was calculated by Bisti revealing that Γ_{ee} exceeds Γ_{ep} if the concentration of excitons exceeds 10^{13} cm^{-3} . In order to compare Γ_{ee} with Γ_{ei} we can use the results of Ziljaev et al. [33]. For pure GaAs it was shown that the value of Γ_{ei} exceeds that of Γ_{ep} by more than an

order of magnitude even when the impurity concentration is lower than 10^{14} cm^{-3} . Therefore, the energy distribution of polaritons predicted by the Bisti's theory can be realized experimentally only in very pure semiconductor crystals, which might be the reason for the lack of any experimental observation of that additional polariton line so far in GaAs. Another possible reason may be connected with exciton screening at high excitation densities. The influence of the exciton screening is greater at greater exciton radii. It is possible that in GaAs with the exciton radii greater than that in AlGaAs the screening at high excitation densities is more important than the exciton–exciton collision process.

4.3. Comparison of the Bisti's theory with experiment, *cw* PL spectra

Using Bisti's theory we calculated the LPB radiation $I(E)$ determining the energetic position and intensity of the additional polariton line as functions of the density (n) and temperature (T_{ex}) of the exciton gas. The values of the permittivity and effective masses of the charge carriers in AlGaAs alloys used in the calculations were taken from Ref. 28. The probability of the nonradiative recombination of excitons, which is a parameter in the calculation, was taken to be $3 \cdot 10^8 \text{ s}^{-1}$ to reach the best agreement between the experimental data and calculation. The energy value at the crossover between exciton and photon dispersion curves as a function of the AlAs fraction was calculated using the AlGaAs band-gap and free exciton binding energy taken from Ref. 34 and Ref. 35, respectively. In order to compare the experimental spectra with calculated data we estimated the concentration of nonequilibrium carriers using the method described in Ref. 28. For this estimation, we took a charge carrier lifetime of 1 ns (evaluated from our time-resolved data) and a carrier diffusion length of $1 \mu\text{m}$ (from Ref. 28). In order to determine the value of T_{ex} , which raises with increasing excitation power, we fitted the high-energy tail of the *X* line by a temperature-dependent exponential function $f(\hbar\omega) = a \exp(-\hbar\omega/kT_{\text{ex}})$, where a is a constant, $\hbar\omega$ is the photon energy, and k is the Boltzmann's constant [36]. As shown in Fig. 3 the temperature of the exciton gas increases from 6 to 20 K within the applied excitation power range.

The experimentally observed and calculated photoluminescence spectra are given in Fig. 6, *a* and Fig. 6, *b*, respectively, showing good accordance. Indeed, the novel *Y* line appears in the calculated spectra at an exciton concentration higher than 10^{13} cm^{-3} in agreement to the experimental data. The width of the *Y* line in the experimental spectra is slightly broader compared to the calculated spectra which is attributed to alloy disorder neglected by the applied theory. The calculated energy position of the *Y* line as a function of the exciton concentration n is given by the logarithmic dependence $\hbar\omega \propto kT \ln n$, which fits the experimental data of Fig. 2 well. Note, however, that the calculated dependence of the *Y* line intensity on the exciton concentration, given by an expression $I_Y \propto n^{1.3} T_{\text{ex}}^{-5/4}$, slightly differs from

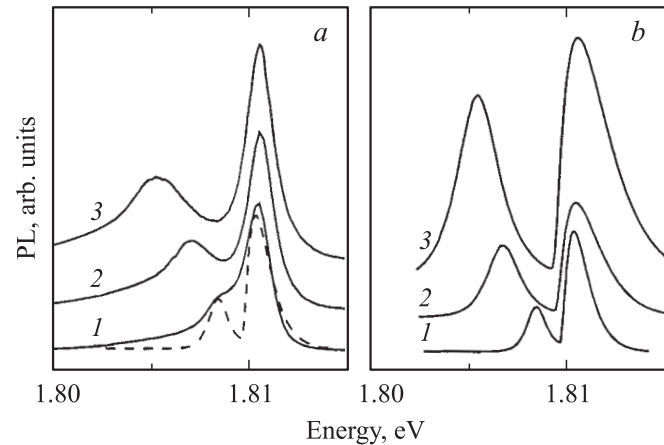


Figure 6. Low temperature photoluminescence spectra: *a* — experimentally observed and *b* — calculated at different exciton concentrations: 1 — $2 \cdot 10^{13} \text{ cm}^{-3}$, 2 — 10^{14} cm^{-3} , 3 — $7 \cdot 10^{14} \text{ cm}^{-3}$. The calculated spectrum at an exciton concentration of $2 \cdot 10^{13} \text{ cm}^{-3}$ is also shown in the left figure as dashed line.

the experimental data. The best fit of the ratio of the *Y* line to *X* line intensity versus the exciton concentration is given by $I_Y/I_X \propto n^{0.1} T_{\text{ex}}^{-5/4}$. Since the intensity of the *X* line is proportional to the exciton concentration [16], the intensity of the *Y* line is described by $I_Y \propto n^{1.1} T_{\text{ex}}^{-5/4}$. We suppose that the difference between the experimental and calculated values of the *Y* line intensity can be explained by two factors: (i) a deviation of the spatial polariton distribution from the uniform distribution assumed by Bisti; and (ii) a deviation of the energy distribution of polaritons from that postulated by Bisti due to the scattering of excitons caused by alloy disorder. In fact, the intensity of the *Y* line decreases when the crystal thickness decreases [15]. Actually, the effective thickness of the crystal is lower than the sample thickness taken in our calculation because the realistic spatial polariton distribution is a decaying function of depth, as shown by Rossin [37]. In addition the extra scattering by alloy disorder, which competes with exciton–exciton scattering, leads to a decrease of the exciton-to-polariton transition rate.

4.4. Kinetics of the polariton emission

The most intriguing result of the time-resolved PL experiment is that the decay curve of the *Y* line shows a biexponential behavior at high excitation powers while it reveals a single exponential decay at the low excitation power. In the latter case the characteristic decay time is half the time constant of the *X* emission, which is typical for a radiation generated by exciton–exciton collisions [38]. We will show that the biexponential behavior at high excitation powers is due to a cooling of the exciton gas after the excitation pulse.

If the exciton-to-polariton transitions are due to collisions of excitons, then the kinetics of the polariton concentration

is described by

$$\frac{dn_p}{dt} = -\frac{n_p}{\tau_p} + B(t), \quad (2)$$

where n_p and τ_p are the concentration and the radiative lifetime of polaritons, respectively, and $B(t)$ is the rate of the exciton-to-polariton transitions due to the exciton–exciton collisions.² The low polariton state density and the low value of the polariton lifetime [6] allow us to neglect the inverse polariton–exciton transitions in expression (2). Since the exciton gas has a Maxwellian energy distribution, which is evidenced by the exponential shape of the high-energy tail of the X line in both the cw and time-resolved PL spectra [39], the rate of the exciton-to-polariton transitions due to the elastic exciton–exciton collisions may be written following Bisti [15] as³

$$B(t) \propto \frac{n_{\text{ex}}^2(t)}{kT_{\text{ex}}(t)} J\left(\frac{\Delta E}{kT_{\text{ex}}(t)}\right) \exp\left(-\frac{\Delta E}{kT_{\text{ex}}(t)}\right), \quad (3)$$

where n_{ex} is the concentration of excitons, ΔE is the difference between the initial and final energies of the excitons, and $J(x)$ is a slowly-varying function of x calculated in Ref. 8. In order to determine the dependence of the exciton temperature T_{ex} on time, we fitted the high-energy tail of the X line in the time-resolved spectra with a temperature-dependent exponential function $f(\hbar\omega) = a \exp(-\hbar\omega/kT_{\text{ex}})$. The variation of the exciton gas temperature (or more specifically, kT_{ex}) with delay time after the laser pulse at the high pulse energy is presented in Fig. 4, *a* by the dotted line. After the formation of an exciton gas, its temperature considerably exceeds the lattice temperature [36,39]. The temperature of the excitons decreases with time due to the exciton–phonon scattering [36]. Two distinct intervals are observed in the decay: (i) for delay time between 200 ps and 700 ps the temperature T_{ex} decreases from about 100 K to 18 K with decreasing exciton density; (ii) for a delay time longer than 700 ps, T_{ex} is equal to 18 K that is close to the lattice temperature of 14 K and hardly changes with time. The same procedure at low pulse intensity shows that T_{ex} , which is about 30 K at the maximum of the laser pulse, becomes close to the lattice temperature within 200 ps. The values of $n_{\text{ex}}(t)$ and ΔE , which are also required for the calculation of the function $B(t)$, have been derived from the experimental data. The concentration $n_{\text{ex}}(t)$ is proportional to the intensity of the X line as shown in Ref. 16, and ΔE can be taken as the value of the red-shift of the Y line. The calculated kinetics of the new polariton line intensity using Eq. (3) is shown in Fig. 4, *a* as dashed curve indicating that the kinetics is well described by the theoretical model. The fast initial decay of the Y line at

² In general, we should include the term, which corresponds to the rate of the exciton-to-polariton transition due to exciton–phonon collisions in expression (1). However, the exciton–exciton collisions become the dominant mechanism of exciton-to-polariton transition at low temperatures and sufficiently high exciton concentrations.

³ See also the calculation of the elastic exciton–exciton scattering rate in microcavities [40].

the high excitation level coincides with the cooling of the exciton gas. When the exciton gas temperature comes close to the lattice temperature, the slope of the Y line decay curve approaches half of the decay time of the X emission.

5. Summary

In conclusion, we have observed a new polariton radiation line in the photoluminescence spectra of ultra-high quality AlGaAs layers. We have shown that this line appears as a result of the exciton-to-polariton transition caused by the elastic exciton–exciton collisions. The rate of the elastic exciton-to-polariton scattering is determined not only by the density of the excitonic gas, but also by its temperature.

Acknowledgments

We acknowledge the support of this work by the Russian Foundation for Basic Research (N 04-02-16774) and by the Graduiertenkolleg „Thin films and non-crystalline materials“ of the Technische Universität Chemnitz.

References

- [1] S.I. Pekar. Zh. Eksp. Teor. Fiz., **33**, 1022 (1957).
- [2] J.J. Hopfield. Phys. Rev., **112**, 1555 (1958).
- [3] *Excitons. Topic in Current Physics*, ed. by K. Cho (Springer, Berlin, 1979) vol. 14.
- [4] C. Weisbuch, R.G. Ulbrich. J. Luminesc., **18/19**, 27 (1979).
- [5] V.V. Travnikov, V.V. Krivolapchuk. Sov. Phys. JETP, **85**, 2087 (1983).
- [6] Yu. Toyozawa. Progr. Theor. Phys., Suppl. **12**, 111 (1959).
- [7] U. Heim, P. Wiesner. Phys. Rev. Lett., **30**, 1205 (1973).
- [8] W.C. Tait, R.L. Weiher. Phys. Rev., **178**, 1404 (1969).
- [9] H. Sumi. J. Phys. Soc. Japan, **41**, 526 (1976).
- [10] R. Ulbrich, C. Weisbuch. Phys. Rev. Lett., **38**, 865 (1977).
- [11] C. Weisbuch, R.G. Ulbrich. Phys. Rev. Lett., **39**, 654 (1977).
- [12] F. Askary, P.Y. Yu. Phys. Rev. B, **31**, 6643 (1985).
- [13] E. Koteles, J. Lee, J.P. Salerno, M.O. Vassell. Phys. Rev. Lett., **55**, 867 (1985).
- [14] C. Klingshirn, H. Haug. Phys. Reports, **70**, 315 (1981).
- [15] V.E. Bisti. Sov. Phys. Sol. St., **18**, 1056 (1976).
- [16] K.S. Zhuravlev, A.I. Toropov, T.S. Shamirzaev, A.K. Bakarov. Appl. Phys. Lett., **76**, 1131 (2000).
- [17] R.P. Seisyan, V.A. Kosobukin, S.A. Vaganov, M.A. Markosov, T.S. Shamirzaev, K.S. Zhuravlev, A.K. Bakarov, A.I. Toropov. Phys. Status Solidi (c), **2**, 900 (2005).
- [18] D.D. Sell, S.E. Stokowski, R. Dingle, J.V. DiLorenzo. Phys. Rev. B, **7**, 4568 (1973).
- [19] T. Steiner, M.L.W. Thewalt, E.S. Koteles, J.P. Salerno. Phys. Rev. B, **34**, 1006 (1986).
- [20] T.S. Shamirzaev, K.S. Zhuravlev, A.I. Toropov, A.K. Bakarov. JETP Lett., **71**, 148 (2000).
- [21] P.W.M. Blom, P.J. van Hall, C. Smit, J.P. Cuypers, J.H. Wolter. Phys. Rev. Lett., **71**, 3878 (1993).
- [22] J.X. Shen, R. Pittini, O. Oka, E. Kurtz. Phys. Rev. B, **61**, 2765 (2000).
- [23] M. Gurioli, P. Borri, M. Colocci et al. Phys. Rev. B, **58**, R 13 403 (1998).

- [24] R.G. Ulbrich. Phys. Rev. B, **8**, 5719 (1973).
- [25] I.V. Belousov, V.V. Frolov. Phys. Rev. B, **54**, 2523 (1996).
- [26] J.X. Shen, R. Pittini, Y. Oka, P.S. Guo, M.C. Tamargo. Appl. Phys. Lett., **75**, 3494 (1999).
- [27] R.T. Phillips, D.J. Lovering, G.J. Denton, G.W. Smith. Phys. Rev. B, **45**, 4309 (1992).
- [28] L. Pavesi, M. Guzzi. J. Appl. Phys., **75**, 4779 (1994).
- [29] O. Akimoto, E. Hanamura. J. Phys. Soc. Japan, **33**, 1537 (1972).
- [30] T.W. Steiner, A.G. Steele, S. Charboneau et al. Sol. St. Commun., **69**, 1139 (1989).
- [31] K.K. Bajaj. Mater. Sci. Eng. B, **79**, 203 (2001).
- [32] Yong-Hoon Cho, T.J. Schmidt, S. Bidnyk, G.H. Gainer, J.J. Song, S. Keller, U.K. Mishra, S.P. DenBaars. Phys. Rev. B, **61**, 7571 (2000).
- [33] Yu.V. Ziljaev et al. Sov. Phys. Sol. St., **28**, 2688 (1986).
- [34] M.El. Allali, C.B. Sorensen, E. Veje, P. Tidemand-Petersson. Phys. Rev. B, **48**, 4398 (1993).
- [35] B. Monemar. Phys. Rev. B, **8**, 5711 (1973).
- [36] H.W. Yoon, D.R. Wake, J.P. Wolfe. Phys. Rev. B, **54**, 2763 (1996).
- [37] V.V. Rossin. Sov. Phys. Sol. St., **31**, 218 (1989).
- [38] R. Huang, F. Tassone, Y. Yamamoto. Phys. Rev. B, **61**, R 7854 (2000).
- [39] D. Robart, X. Marie, B. Baylac et al. Sol. St. Commun., **95**, 287 (1995).
- [40] F. Tassone, Y. Yamamoto. Phys. Rev. B, **59**, 10830 (1999).

Редактор Т.А. Полянская